

**Steady transcritical flow over a hole: parametric map of solutions of the forced Korteweg-de Vries equation**

Bernard K. Ee,<sup>1, a)</sup> R. H. J. Grimshaw,<sup>2, b)</sup> D-H. Zhang,<sup>3, c)</sup> and K. W. Chow<sup>3, d)</sup>

<sup>1)</sup>*Department of Mathematics and Statistics,  
King Fahd University of Petroleum and Minerals,  
Dhahran 31261, Kingdom of Saudi Arabia*

<sup>2)</sup>*Department of Mathematical Sciences,  
Loughborough University, UK*

<sup>3)</sup>*Department of Mechanical Engineering,  
University of Hong Kong,  
Pokfulam Road, Hong Kong*

(Dated: 29 January 2010)

Transcritical flow of a stratified fluid over an obstacle, or through a contraction, can be modeled by the forced Korteweg - de Vries equation, which describes a balance between weak nonlinearity, weak dispersion and small forcing effects. Here we seek steady solutions with constant, but different amplitudes upstream and downstream of the forcing region. Our interest is in the case when the forcing has negative polarity, that is it can represent a hole. The effects of the width of the hole and the amplitude of the hole on these steady solutions are investigated.

---

<sup>a)</sup>Electronic mail: kwee@kfupm.edu.sa

<sup>b)</sup>Electronic mail: R.H.J.Grimshaw@lboro.ac.uk

<sup>c)</sup>Electronic mail: dzhang@hkucc.hku.hk

<sup>d)</sup>Electronic mail: kwchow@hkusua.hku.hk

## I. INTRODUCTION

Stratified flows over an obstacle or through a contraction have relevance in both oceanographic and engineering contexts. The textbook by Baines<sup>1</sup> describes the general theory of stratified flow over topography as well as many applications. When the oncoming flow is close to critical, nonlinear effects become particularly important, and the forced Korteweg-de Vries (KdV) equation is often used as a suitable model to describe transcritical flow over an obstacle or through a contraction, see Grimshaw and Smyth<sup>2</sup> and Clarke and Grimshaw<sup>3</sup> respectively. The forced KdV equation is

$$A_t + cA_x + rAA_x + sA_{xxx} = -G_0f_x. \quad (1)$$

Here  $A(x, t)$  is the amplitude of the relevant linear long wave mode, where  $x, t$  are the spatial and time variables respectively.  $c$  is the linear long wave phase speed in the reference frame of the obstacle, The coefficients  $r, s$  are determined by the background stratification,  $G_0$  is a measure of the forcing magnitude, and  $f(x)$  is a projection of the obstacle onto the relevant long wave mode. In the work of Grimshaw and Smyth<sup>2</sup> and Clarke and Grimshaw<sup>3</sup>, and in many other works on transcritical flow (see the references below) the forcing term was localized, and the emphasis was on the development of upstream and downstream undular bores, emanating from a local hydraulic flow over the obstacle.

Recently Ee and Clarke<sup>4</sup> investigated the family of steady hydraulic flows over a localized obstacle of positive polarity ( $\gamma < 0$ ) in the framework of the steady forced KdV equation. They obtained the family of all steady dispersive hydraulic solutions as a parametric map  $\Delta(\gamma)$ , thus extending the parametric relationships obtained by Grimshaw and Smyth<sup>2</sup> which were non-dispersive or for a  $\delta$ -function forcing term. By treating the steady version of (3) as a three-dimensional dynamical system, they developed a numerical procedure in which a shooting algorithm was implemented alongside a minimization algorithm in order to obtain the steady dispersive hydraulic solution. Then a branch-following algorithm was developed to obtain the desired parametric relationship. In this paper we extend that study by considering obstacles with negative polarity ( $\gamma > 0$  (that is, a hole) and we also take account of the obstacle width as an additional parameter.

At this juncture, we shall review some of the relevant papers which discuss transcritical flow over an obstacle, with a particular focus on the effect of the obstacle width, and on the steady hydraulic solutions. Zhang and Chwang<sup>5</sup> used numerical simulations of the full Euler

equations for the equivalent problem of an underwater obstacle traveling at a transcritical speed in a two-dimensional shallow water channel. They found that the phenomenon of the successive generation of upstream advancing solitary waves was dependent on the dimensions of the moving obstacle. In particular, they showed that as the blockage coefficient of the obstacle increases, the amplitude of these solitary waves increases while the period at which the generation of these solitary waves occurs decreases. In a subsequent paper<sup>6</sup>, they explored, again through numerical simulations, the effect of the width of the obstacle. In a limiting configuration they simulated transcritical flow over either a positive step (that portion of the forcing which is monotonically increasing), or a negative step (that portion of the forcing which is monotonically decreasing). Their results showed that a positive step generates an upstream-propagating undular bore whereas a negative step generates a downstream-propagating undular bore. This implied that the upstream and downstream wavetrains generated by transcritical flow over a localized obstacle may be generated by separated processes.

Grimshaw et al.<sup>7</sup> investigated transcritical flow over a step in the framework of the forced KdV equation (3). Asymptotic solutions consisting of steady, hydraulic solutions in the vicinity of an isolated step were constructed, and matched with upstream and downstream undular bores as appropriate. For a positive forcing term, that is a positive step followed by a negative one, they confirmed the numerical results of Zhang and Chwang<sup>6</sup> that positive and negative steps generated upstream and downstream propagating undular bores respectively. Solutions over long, but finite obstacles were also constructed numerically, and again agreed with analogous results from the fully nonlinear simulations. They next extended this work to the case of a hole<sup>8</sup>, that is a combination of a negative step followed by a positive step. Negative and positive steps were shown to generate downstream and upstream undular bores. However, unlike the case for positive forcing<sup>7</sup>, these wavetrains were found to interact over the hole and the long-time behaviour was not determined. This is an issue we address in this present paper.

Dias and Vanden-Broeck<sup>9</sup> considered steady transcritical free surface flows over a localized obstacle, in scenarios where they were supercritical upstream but tended to wave solutions far downstream. They used a combination of weakly nonlinear analysis based on the steady forced KdV equation, and fully nonlinear numerical solutions. Hydraulic flow solutions, where the downstream waves disappear, is a limiting case. In their subsequent work<sup>10,11</sup>,

they investigated the analogous dynamics of interfacial waves for flows of two contiguous homogeneous fluids with different densities and layer thickness over an obstacle. Later, they considered the flow past two obstacles of arbitrary shape and showed that the resulting steady solution to the forced KdV equation was characterised by supercritical flow on one side of the obstacle and a train of waves trapped between these two obstacles<sup>12</sup>. Such a configuration of obstacles is relevant to this paper as it is similar to our definition of a hole. They found that an increase in the distance between the obstacles (equivalent to our increasing the width of the forcing) merely increases the number of waves without changing the lengths or amplitudes of the existing waves. Binder et al investigated steady hydraulic solutions over two localized obstacles of differing magnitudes<sup>13</sup> and over a step<sup>14</sup>. Again, they used analysis of the forced KdV equation combined with numerical solutions of the fully nonlinear steady Euler equations.

In this paper we seek to complement these works by describing the relationship between the magnitude and width of our hole-like forcing and the formation of the trapped waves. We shall use the framework of the steady forced KdV equation, and use both theoretical analyses and numerical solutions. Specifically we choose a forcing term

$$f(x) = \frac{1}{2} \tanh\left(\xi\left[x - \frac{L}{2}\right]\right) - \frac{1}{2} \tanh\left(\xi\left[x + \frac{L}{2}\right]\right), \quad (2)$$

where  $L$  is the separation between the front and rear steps and  $1/\xi$  measures the width of these steps. The forcing term (2) is symmetric and centered at  $x = 0$  where  $x < -\frac{L}{2}$  and  $x > \frac{L}{2}$  denote the upstream and downstream regions respectively.

In Section II, the problem we shall consider is presented in canonical form to identify the relevant parameters. In Section III, we consider the case of piece-wise constant forcing when an analytical solution can be found using phase-plane analysis. In Section IV, a brief outline of the numerical method is followed by a discussion of our numerical results for the smooth forcing term (2). Finally, we conclude with a summary of our key results in Section V.

## II. FORMULATION

We now transform the fKdV equation (1) to a canonical form, so that the problem considered will contain only three parameters. Thus let  $\tilde{x} = \xi x$ ,  $\tilde{t} = \xi \delta r t / 6$ ,  $A(x, t) =$

Steady transcritical flow over a hole

$\delta B(\tilde{x}, \tilde{t}) + A_0, \tilde{L} = \xi L$  and where  $r\delta = 6s\xi^2$  and  $A_0$  is a characteristic upstream amplitude.

Then  $B$  satisfies the fKdV equation

$$B_t + \Delta B_x + 6BB_x + B_{xxx} = -\gamma f_x. \quad (3)$$

$$\text{where } \Delta = \frac{6(c + rA_0)}{r\delta}, \quad \gamma = \frac{6G_0}{r\delta^2}, \quad (4)$$

and the tildes are omitted for the scaled independent variables  $x$  and  $t$ . Here  $\Delta$  and  $\gamma$  represent the detuning and forcing parameters respectively. With this re-scaling the forcing term (2) then becomes

$$f(x) = \frac{1}{2} \tanh\left(x - \frac{L}{2}\right) - \frac{1}{2} \tanh\left(x + \frac{L}{2}\right), \quad (5)$$

where  $L$  is the third parameter (again the tilde has been omitted) which we shall vary independently in order to investigate its effect on the parametric map  $\Delta(\gamma)$ . Note that  $-1 \leq f(x) \leq 0$ , there is a minimum at  $x = 0$  where  $f(0) = -1$ , and  $f \rightarrow 0$  as  $|x| \rightarrow \infty$ . When  $\gamma > 0$  this forcing term represents a hole, and is our main concern in this paper.

As stated in Section I, our concern here is with the steady dispersive hydraulic solutions. Hence, we set the time derivative term in (3) to zero. One integration then yields

$$\Delta B + 3B^2 + B_{xx} = -\gamma f(x), \quad (6)$$

where it has been assumed without loss of generality that the far upstream amplitude is  $B = 0$ ; this can always be achieved by an appropriate choice of  $A_0$  in the re-scaling described above. Next, in the far-field where there is no forcing term (6) reduces to

$$\Delta B + 3B^2 + B_{xx} = 0, \quad (7)$$

which has two critical points  $B = 0$  and  $B = -\Delta/3$ . For  $\Delta > 0$ , these correspond respectively to a centre and a saddle point. This is reversed for  $\Delta < 0$ . Since we can transform the latter case to the former through the addition of a mean level, we can therefore assume that  $\Delta \geq 0$  for steady hydraulic solutions. Hence we can now impose the boundary conditions

$$B \rightarrow 0 \quad \text{as } x \rightarrow -\infty, \quad B \rightarrow -\frac{\Delta}{3} \quad \text{as } x \rightarrow \infty. \quad (8)$$

Thus the steady flow solutions that we seek are subcritical upstream and supercritical downstream, leading to asymmetric dispersive hydraulic solutions of the fKdV equation. A typical

representation of the two steady hydraulic solutions over a hole and a plateau, including the latter forcings are given in Figures 1 and 2 respectively.

In summary, we seek steady dispersive analogues of hydraulic flows that solve (3) and the boundary conditions (8), where the forcing term  $f(x)$  given by ((5)). The set of all such solutions can be described by a parametric relationship  $F(\gamma, \Delta, L) = 0$ . Thus, for each given width  $L$  of the hole, a solution exists only if  $\Delta = \Delta(\gamma)$ . Our aim is to obtain a complete description of this parametric map for all  $\gamma > 0$ . In particular, in relation to the study by Grimshaw et al<sup>8</sup> of unsteady transcritical flow over a hole, we would like to address the following questions:

- How does the parametric map and the corresponding set of steady hydraulic solutions compare with those found in Ee and Clarke<sup>4</sup> for the case  $\gamma < 0$ .
- How does the separation distance  $L$  between the front and rear steps of the forcing term influence the parametric map  $\Delta(\gamma)$ ?
- How does the set of steady hydraulic flows vary along the parametric map  $\Delta(\gamma)$ ?
- What is the relationship between  $L$  and the existence of the trapped waves over the hole?

### III. PIECE-WISE CONSTANT FORCING

In order to obtain some insight into the numerical solutions we shall describe in Section IV, we shall, in this section, replace the forcing term (5) by a piece-wise constant forcing term where  $f(x) = -1, -L/2 < x < L/2$  and  $f(x) = 0$  elsewhere. Then on the upstream side, the boundary condition (8) implies that

$$B = 0 \quad \text{for} \quad x < -\frac{L}{2}. \quad (9)$$

Consequently, we can set matching conditions at  $x = -L/2$ ,

$$B = 0, \quad B_x = 0 \quad \text{as} \quad x \rightarrow -\frac{L}{2}(+). \quad (10)$$

These are sufficient to determine the solution, as a function of the parameters  $\Delta, \gamma$  and also  $L$ . But downstream, a solitary wave is permitted, and so we can assume that the solution

Steady transcritical flow over a hole

is then given by

$$B = -\frac{\Delta}{3} + \frac{\Delta}{2} \operatorname{sech}^2\left(\frac{\Delta^{1/2}}{2}(x - L/2) + \theta\right), \quad (11)$$

in terms of one unknown constant  $\theta$ . The matching conditions at  $x = L/2$  then become

$$B = -\frac{\Delta}{3} + \frac{\Delta}{2} \operatorname{sech}^2\theta, \quad B_x = -\frac{\Delta^{3/2}}{2} \operatorname{sech}^2\theta \tanh\theta \quad \text{as } x \rightarrow \frac{L}{2}(-). \quad (12)$$

These generate two equations for  $\theta, \Delta, \gamma$ , for each given  $L$ . Elimination of  $\theta$  yields the parametric curve  $\Delta = \Delta(\gamma)$  as  $x \rightarrow L/2(-)$ , that is

$$B_x^2 = \left(B + \frac{\Delta}{3}\right)^2 \left(\frac{\Delta}{3} - 2B\right) \quad (13)$$

must hold there. Indeed, this is the defining equation for the homoclinic orbit in the  $B_x - B$  phase plane in  $x > L/2$ . Note that we must have  $B(x = L/2) > 0$ , indicating that the critical point  $B = -\Delta/3, B_x = 0$  at infinity must be approached from inside the homoclinic orbit. These remarks apply to both positive and negative forcing in  $-L/2 < x < L/2$ .

### A. Negative forcing

Now suppose that  $\gamma > 0$  corresponding to negative forcing. First we examine this case in the phase plane following the approach of Vanden-Broeck, Dias and collaborators<sup>12,14</sup>. The phase plane in  $x < -L/2, x > L/2$  is shown as the blue curve in Figure 3, where there is a centre at the origin, and a saddle point at  $B = -\Delta/3, B_x = 0$ . The direction of increasing  $x$  is clockwise.

Here, the task is to connect the centre with the saddle point using the orbits in the phase plane for  $-L/2 < x < L/2$ . The critical points in the hole are given by

$$B_x = 0, \quad 6B = -\Delta \pm (\Delta^2 + 12\gamma)^{1/2}. \quad (14)$$

We see that since  $\gamma > 0$  the centre is moved in the direction of positive  $B$ , while the saddle point is moved in the direction of negative  $B$ . The homoclinic orbit (the green curve) in  $-L/2 < x < L/2$  must lie outside the homoclinic orbit (the blue curve) for  $x > L/2$ . We can use that periodic orbit (the red curve) from the origin ( $x = -L/2$ ) in the clockwise direction, until it meets the homoclinic orbit at  $x = X$  say. However, in general  $X \neq L/2$ , and so the values of  $\Delta, \gamma$  must be adjusted until  $X = L/2$ . It may be necessary to go around the periodic orbit several times, which corresponds to several wave crests in the hole. Note

Steady transcritical flow over a hole

that  $0 < B < \Delta/6$  at the intersection point, and that an intersection in the quadrant where  $B_x > 0, < 0$  corresponds in  $x > L/2$  to a a partial solitary wave with a crest, or to a suppressed solitary wave respectively.

This phase plane analysis can now be done explicitly in terms of cnoidal waves in the region  $-L/2 < x < +L/2$ ,

$$B = d + a \operatorname{cn}^2\left(\beta\left(x + \frac{L}{2} - x_0\right); m\right), \quad (15)$$

$$\text{where } a = 2\beta^2 m, \quad \Delta = -6d - \frac{2a}{m}(2m - 1), \quad \gamma = \Delta d + 3d^2 + \frac{a^2}{m}(1 - m). \quad (16)$$

Here  $\operatorname{cn}(u; m)$  is the Jacobi elliptic function of modulus  $m$ . Since  $0 < m < 1$ ,  $a > 0$ . The phase plane in  $-L/2 < x < L/2$  is given by

$$B_x^2 + 2B^3 + \Delta B^2 = 2\gamma B + C, \quad C = 2d^3 + \Delta d^2 - 2\gamma d. \quad (17)$$

This solution contains two arbitrary constants, say  $d, x_0$ . The boundary conditions at  $x = -L/2$  can be met either by  $x_0 = 0, d = -a$  or by  $\beta x_0 = K(m), d = 0$ , where  $K(m)$  is the complete elliptic integral of the first kind. These lead respectively to the conditions

$$\gamma = -\frac{2a^2}{m}, \quad \Delta = \frac{2a}{m}(m + 1); \quad \text{or} \quad \gamma = \frac{a^2}{m}(1 - m), \quad \Delta = -\frac{2a}{m}(2m - 1). \quad (18)$$

Since  $\gamma > 0$ , the first case is not allowed and only the second case is relevant here for negative forcing, where also it is required that  $0 < m < 1/2$ . Note that now  $C = 0$ . Next we can combine the expressions for  $B_x^2$  (17) in  $-L/2 < x < L/2$  in the limit as  $x \rightarrow L/2(-)$  with the matching condition obtained above to find that

$$2\gamma B(x = L/2(-)) = \frac{\Delta^3}{27}. \quad (19)$$

This now yields an explicit formula for the parametric curve, namely that

$$2\gamma a \operatorname{cn}^2(\beta L - K(m); m) = \frac{\Delta^3}{27}, \quad (20)$$

where  $\gamma, \Delta$  are defined in terms of  $a, m$  by the second set of expressions in (18). This formula can then be written as

$$\frac{27m^2(1 - m)}{4(2m - 1)^3} \operatorname{cn}^2(\beta L - K(m); m) = -1. \quad (21)$$

This expression determines  $\beta L$  in terms of  $m$ , say  $\beta L = F(m)$ . Note that since  $0 \leq \operatorname{cn}^2(\cdot) \leq 1$ , the expression (21) can only have solutions in the range  $0.5 > m > 0.2$ . Then finally

the expression  $a = 2\beta^2 m$  yields the relation  $\Delta = \Delta(\gamma)$  as a parametric plot with  $m$  as the parameter,

$$\tilde{\gamma} = \gamma L^4 = 4F^4(m)m(1-m), \quad \tilde{\Delta} = \Delta L^2 = 4F^2(m)(1-2m) \quad (22)$$

Importantly,  $F(m)$  is multi-valued, since we can write  $\beta L = (2n+1)K(m) \mp F_0(m)$ ,  $n = 0, 1, 2, \dots$  where  $F_0(m)$  is that solution such that  $0 < F_0(m) < K(m)$ . The integer  $n$  determines the number of complete trapped waves in  $-L/2 < x < L/2$ , and the alternate signs  $\mp$  correspond to  $B_x(x = L/2) > 0, < 0$ , corresponding to partial solitary waves with crests, or to suppressed solitary waves respectively in  $x > L/2$ . A typical plot is shown in Figure 4. Note that as well as being multi-valued in  $\gamma$  for a fixed  $\Delta$  as  $n$  increases, the curves are also multi-valued in  $\Delta$  for a fixed  $\gamma$ , most evident in the plots for  $n \geq 2$ .

## B. Positive forcing

Although the case of a hole is our main concern in this paper, it is useful to revisit here the case when  $\gamma < 0$ , that is the case of a positive forcing term previously considered by Ee and Clarke<sup>4</sup>. The phase plane analysis can again be applied, but there are now major differences. First, in  $-L/2 < x < L/2$ , there are no critical points when  $\Delta^2 < -12\gamma$ . In this case the phase plane typically has the structure shown in Figure 5. Hence the orbit from the origin (the red curve) which intersects the homoclinic orbit outside the forcing cannot be a periodic solution, and hence there are no waves in the forcing region. Instead it is that portion of the unbounded orbit which lies in  $B_x < 0, B < 0$ . In this case the intersection is in the same quadrant, and hence always  $\theta > 0$  and it is the case of a suppressed solitary wave in  $x > L$ .

If there are critical points, the centre is moved towards the direction of decreasing  $B$ , and the saddle point is moved in the direction of increasing  $B$ , in contrast to the case when  $\gamma > 0$ . There are two possible scenarios. If  $-16\gamma > \Delta^2 > -12\gamma$ , then the homoclinic orbit (the green curve) in  $x_p - L/2 < x < x_p + L/2$  lies entirely in the region  $B < 0$ . The situation is similar to that of 5. The connecting curve cannot be part of a periodic orbit. But if  $\Delta^2 > -16\gamma$ , then the homoclinic orbit (the green curve) in  $x_p - L/2 < x < x_p + L/2$  encloses the origin, but lies entirely inside the homoclinic orbit outside the forcing region. In this case there are no steady solutions at all.

The conclusion that there can be no cnoidal wave solutions when  $\gamma < 0$  can also be shown directly using a similar analysis to that in Section III A. Instead, to find the solution when allowed ( $\Delta^2 < -16\gamma$ ), we must use the unbounded solutions of the governing equation as follows. We now seek that solution which is such that  $B = B_x = 0$  at  $x = -L/2$  and such that  $2\gamma B = \Delta^3/27$  at  $x = L/2$ . Note that now with  $\gamma < 0$ , necessarily we must have that  $B(x = L/2) < 0$ , as is clear from the phase plane plots. Formally this is given by the expression

$$\int_0^{\Delta^3/54\gamma} \frac{dB}{(2\gamma B - \Delta B^2 - 2B^3)^{1/2}} = -L \quad (23)$$

For the integrand to be defined in  $B < 0$ , we must have that  $\Delta^2 < -16\gamma$ , consistent with the phase plane analysis. In normalized form, the above integral becomes

$$\int_0^{1/54\Gamma} \frac{db}{(2b^3 - b^2 + 2\Gamma b)^{1/2}} = \Delta^{1/2} L \quad (24)$$

where  $\Gamma = -\gamma/\Delta^2 > 1/16$ . This integral defines the parametric curve  $\Delta = \Delta(\gamma)$  for each fixed  $L$ . We note that the phase plane analysis reveals that these solutions are monotonic with  $B_x < 0, B < 0$  corresponding to a suppressed solitary wave in  $x > L/2$ . This agrees with the results for the steady monotonic solutions in Ee and Clarke<sup>4</sup>.

#### IV. NUMERICAL SOLUTIONS

We now turn to our numerical results for the smooth forcing term (5) where for convenience, the forcing centre is shifted from  $x = 0$  to  $x=x_p$ . Let  $B_u$  denote the far-field upstream amplitude and  $B_d$  denote the far-field downstream amplitude. As discussed above in Section II we seek steady hydraulic solutions such that  $B_u = 0, B_d = -\Delta/3$  and the gradients of the amplitude in the far-field is  $dB_u/dx, dB_d/dx = 0$  respectively. For given  $\gamma, L$  this only occurs for a particular  $\Delta$ , which then leads to a parametric curve  $\Delta(\gamma)$  for each given  $L$ .

The numerical procedure outlined in Ee and Clarke<sup>4</sup> was modified and implemented to solve (6) with the forcing term given by (5) for solutions that are generally asymmetric, dispersive hydraulic flows. A summary of the numerical procedure follows, more details can be found in our previous paper.

- Shoot from the centre ( $B_u$ ) to a saddle point ( $B_d$ ) using the Runge Kutta method of RK(4,5).

- Apply a minimization algorithm to obtain a minimum  $\Delta$  so that  $B_d$  lies within the homoclinic orbit.
- Insist on the constraints of exponential decay to remove downstream solitary waves appended to the steady dispersive hydraulic solution.
- Employ a branch-following algorithm to obtain the parametric curve  $\Delta(\gamma)$ .

The branch-following algorithm was initiated from the trivial ( $\gamma = 0$ ) and solitary wave solutions ( $\gamma \neq 0$ ) where  $\Delta = 0$ .

The branch-following algorithm was slightly modified to be initiated from the previously computed value of  $\Delta$  which is a local minimum of the parametric curve  $\Delta(\gamma)$ .

### A. Negative forcing

In Figure 6, we obtain the parametric maps for various values of  $L$  and observe many loops in them. This is consistent with the piece-wise forcing case discussed in Section III A, and we can see the qualitative similarity between Figures 4 and 6. But we note that although the multi-valued property for a fixed  $\Delta$  as  $\gamma$  and  $n$  increase is present for this smooth forcing (5), we do not find here the multi-valued behaviour for a fixed  $\gamma$  seen for the piece-wise forcing case. We define the loop width as the distance between the two adjacent local minima of the parametric map. The following observations can be made from the latter figure:

- (i) For a given value of  $L$ , the loop width increases as  $\gamma$  increases.
- (ii) As  $L$  increases, the width of the loops decreases while the frequency of the loops increases.
- (iii) The slope of the parametric map connecting the local minimum and then the local maximum decreases as  $\gamma$  increases.
- (iv) The local minima in all the parametric maps correspond to weak solitary wave solutions, i.e.  $\Delta$  is small,  $O(0.1)$ .

Note that the same loop-behaviour was found in our previous paper<sup>4</sup> for a localized forcing term. This allows us to characterize the nature of the parametric map for steady dispersive

hydraulic solutions to the forced KdV equation for all forcings so long as they are symmetric and confined. The main differences here are, first, no numerical solitary wave solution was found in the range of  $\gamma$  considered, and second, there are a lot more loops in our parametric map. We suggest that it is the separation distance between the front and rear steps of a hole, given by  $L$ , that is responsible for the multiple loops, as suggested by the theoretical analysis obtained in the Section III A.

To relate the observations (i) to (iv) to the steady hydraulic solution profiles, we first consider how these solutions change with respect to  $\gamma$  over a single loop. We have different markers to see this and they are given by points (a) to (f) along a single loop shown in Figure 7. Although the magnitudes of the steady dispersive hydraulic solutions will obviously vary from loop to loop, the qualitative behaviour within each loop was found to be the same. The hole is defined over  $x \in [x_p - L/2, x_p + L/2]$  where  $x_p$  is the center of the forcing and  $x_p = 64$ .

From points (a) to (b), a trapped wave (identified by a small peak) begins to form at the positive step (at approximately  $x = 74$ ) as soon as  $\Delta$  increases from the first local minimum in the loop. Note that as this occurs, the far-field downstream amplitude decreases (becoming more negative) and the magnitude of the trapped waves decreases. Compression of the existing trapped waves also begins to occur to make room for the new one being created. From points (b) to (d), this new trapped wave soon matches the same amplitude as the previous trapped waves in the hole. From points (d) to (f), we then observe that the magnitude of the ensemble of trapped waves will increase as  $\Delta$  decreases. We note that the observations described here concerning the generation of the trapped waves support the conclusion that the amplitude of a trapped wave being generated increases with the magnitude of the forcing<sup>5</sup>.

These results suggest that so long as  $L$  is sufficiently large, trapped waves will be formed in the hole. After a long time (the steady-state scenario), the hole (regardless of the magnitude of  $\gamma$ ) contributes to the formation of trapped waves which result from the interaction of two wavetrains, one that propagates downstream from a negative step and the other which moves upstream from a positive step. These were previously discussed in a series of time evolution of wave profiles<sup>8</sup>.

As  $L$  increases, we can see that the hole is wider and hence possesses a greater capacity to accommodate these trapped waves. This explains why we observe a decrease in the width

and an increase in the frequency of these loops in the parametric map as shown in Figure 6. As  $\gamma$  increases in magnitude, the width of the loops increases. This suggests that the finite length of the hole will at some stage slow down the process of forming new trapped waves in the hole.

Another issue is whether there is a value of  $L$  in which no trapped waves can be found in the hole. Since the values of  $L$  considered so far show trapped waves forming in the hole, we choose a sufficiently small value of  $L$  to demonstrate this case as shown in Figure 8 and we chose  $L = 2$ . As observed in the latter figure, we observe that some disturbances is being generated by the positive step, as shown in point (d). However, this disturbance does not become a trapped wave as seen in Figure 7 as  $\Delta$  increases along the parametric map.

Instead, the steady hydraulic solution profile merely widens in the vicinity of the hole with no trapped waves featured as  $\gamma$  increases. This supports previously discussed observations that, for a hole of narrow width, the waves emitted from a negative step of the hole would initially propagate downstream but would then get pushed by the upstream propagating waves emitted by the positive step<sup>6</sup>. As a result, no waves are trapped in such a hole.

On the other hand for a sufficiently wide hole, the waves emitted from the positive step would be unable to push the waves emitted from the negative step resulting in waves trapped in the hole. These results again support our view that  $\gamma$  seeks to spur the formation of a trapped wave but it is restricted by  $L$ . Furthermore, we see that the parametric map and the resulting continuum of steady hydraulic solutions gradually match that obtained for the bell-shaped forcing<sup>4</sup>. This is consistent, since the only difference between our forcing and that of the localized forcing term in Ee and Clarke<sup>4</sup> is the presence of a separation distance  $L$ .

## B. Positive forcing

In Figure 9, we obtain parametric maps for different various values of  $L$  and observe the arcs have the relationship  $|\gamma| \propto \Delta^2$ . For a fixed value of  $\gamma$ , the value of  $\Delta$  increases as  $L$  increases. We note that there appears to be an upper limit in which the parametric relationships for  $\gamma < 0$  appear to be bounded above. This is supported by the theoretical analysis done in Section III B. In addition, the steady monotonic solutions shown in Figure 10 indicate that the magnitude of the far-field downstream amplitude increases as  $|\gamma|$

increases. At the same time, it supports the notion that no steady solutions exist in which cnoidal waves can be found in the forcing region.

## V. CONCLUSION

In this paper, we have investigated the transcritical flow of a stratified fluid over an obstacle or through a contraction, in the framework of the forced KdV equation. Our main concern is with the steady hydraulic solutions which form over a hole. Our main finding is that as long as the hole is wide enough trapped waves are formed over the hole.

We stress that the parametric maps  $\Delta = \Delta(\gamma)$  for each hole width  $L$  that describes the set of steady hydraulic solutions are given in terms of the re-scaled parameters  $\Delta$ ,  $\gamma$  and  $L$  (ref. (4)). Thus in order to relate the present results to the unsteady solutions obtained by Grimshaw and Smyth<sup>2</sup>, and Grimshaw et al<sup>7,8</sup>, we note that the upstream elevation  $A_0$  in these papers can also be expressed as a function of  $\Delta$  and  $\gamma$ . We summarize our key results as follows:

- Parametric maps  $\Delta(\gamma)$  which describe the set of steady state hydraulic solutions that can be formed for flow over a hole in the framework of the forced KdV equation
- The description of the trapped waves that form over sufficiently wide holes.
- For a sufficiently wide hole, each loop in the parametric map  $\Delta(\gamma)$  denotes the formation of a trapped wave inside the hole. This extends the analysis of Dias and Vanden Broeck<sup>12</sup>.
- If the separation distance  $L$  is too small, then a widening of the steady hydraulic solution occurs with no trapped waves found over the hole.
- The effect of the separation distance between the front and rear steps of the hole  $L$  on the formation of the steady state solutions is to increase the capacity to accommodate these trapped waves.
- The effect of the magnitude of the forcing  $\gamma$  is to enhance the formation of the trapped waves in the steady state solutions but this capacity is restricted by  $L$  as above.

The approach being undertaken in this paper differs from that of Grimshaw et al.<sup>8</sup> in that we do not consider how the wave profiles evolve in time. Instead, in effect, we take the limit  $t \rightarrow \infty$ , and seek the allowed set of possible steady state solutions. Our results upport the numerical observations of the latter paper.

Dias and Vanden-Broeck<sup>12</sup> showed that trapped waves could be formed between two separated obstacles of positive polarity, using numerical simulations of the fully nonlinear steady equations for water waves combined with a phase-plane analysis of the forced KdV equation. Further, as shown by Ee and Clarke<sup>4</sup>, it is possible to construct asymmetric periodic solutions, one only needs to draw a horizontal line through the parametric maps given in Figure 6. The intersection of the  $\Delta(\gamma)$  curve then gives dispersive hydraulic solutions with identical downstream levels. Thus, we can theoretically construct solutions with non-matching pairs that involve either a combination of two holes of different magnitudes or a combination of a hole and a plateau. An example of the latter case is shown in Figure 11.

To determine whether the steady hydraulic solutions found here can be realized in practice requires a long-time numerical integration of the unsteady forced KdV equation. Another approach would be to investigate the nonlinear stability characteristics of the steady hydraulic solutions. These aspects are the subject of our future work.

## ACKNOWLEDGMENTS

B. K. Ee acknowledges the kind and generous hospitality of the Department of Mechanical Engineering, University of Hong Kong extended to him during his research visits which helped to facilitate the collaboration that led to the production of this article.

## REFERENCES

- <sup>1</sup>P. G. Baines, *Topographic Effects in Stratified Flows* (Cambridge University Press, 1998).
- <sup>2</sup>R. H. J. Grimshaw and N. Smyth, “Resonant flow of stratified fluid over topography,” *J. Fluid Mech.* **169**, 429 (1986).
- <sup>3</sup>S. R. Clarke and R. H. J. Grimshaw, “Resonantly generated internal waves in a contraction,” *J. Fluid Mech.* **274**, 139 (1994).
- <sup>4</sup>B. K. Ee and S. R. Clarke, “Weakly Dispersive Hydraulic Flows in a Contraction - Parametric Solutions and Linear Stability Analysis,” *Phys. Fluids* **19**, 055601 (2007).
- <sup>5</sup>D. H. Zhang and A. T. Chwang, “On the solitary waves forced by underwater moving objects,” *J. Fluid Mech.* **389**, 119 (1999).
- <sup>6</sup>D. H. Zhang and A. T. Chwang, “Generation of solitary waves by forward- and backward-step bottom forcing,” *J. Fluid Mech.* **432**, 341 (2001).
- <sup>7</sup>R. H. J. Grimshaw, D. H. Zhang, and K. W. Chow, “Generation of solitary waves by transcritical flow over a step,” *J. Fluid Mech.* **587**, 235 (2007).
- <sup>8</sup>R. H. J. Grimshaw, D. H. Zhang, and K. W. Chow, “Transcritical flow over a hole,” *Stud. Appl. Math.* **125**, 235 (2009).
- <sup>9</sup>F. Dias and J. M. Vanden-Broeck, “Generalised critical free surface flows,” *J. Engrg Math.* **42**, 291–301 (2002).
- <sup>10</sup>F. Dias and J. M. Vanden-Broeck, “Steady two-layer flows over an obstacle,” *Phil. Trans. R. Soc. Lond. A* **360**, 2137–2154 (2002).
- <sup>11</sup>F. Dias and J. M. Vanden-Broeck, “Two-layer hydraulic falls over an obstacle,” *Eur. J. Mech. B Fluids* **23**, 879–898 (2004).
- <sup>12</sup>F. Dias and J. M. Vanden-Broeck, “Trapped waves between submerged obstacles,” *J. Fluid Mech.* **509**, 93–102 (2004).
- <sup>13</sup>B. J. Binder, J.-M. Vanden-Broeck, and F. Dias, “Forced solitary waves and fronts past submerged obstacles,” *Chaos* **15**, 037106 (2005).
- <sup>14</sup>B. J. Binder, F. Dias, and J.-M. Vanden-Broeck, “Steady free-surface flow past an uneven channel bottom,” *Theor. Comput. Fluid Dyn.* **20**, 125 (2006).

# Steady transcritical flow over a hole

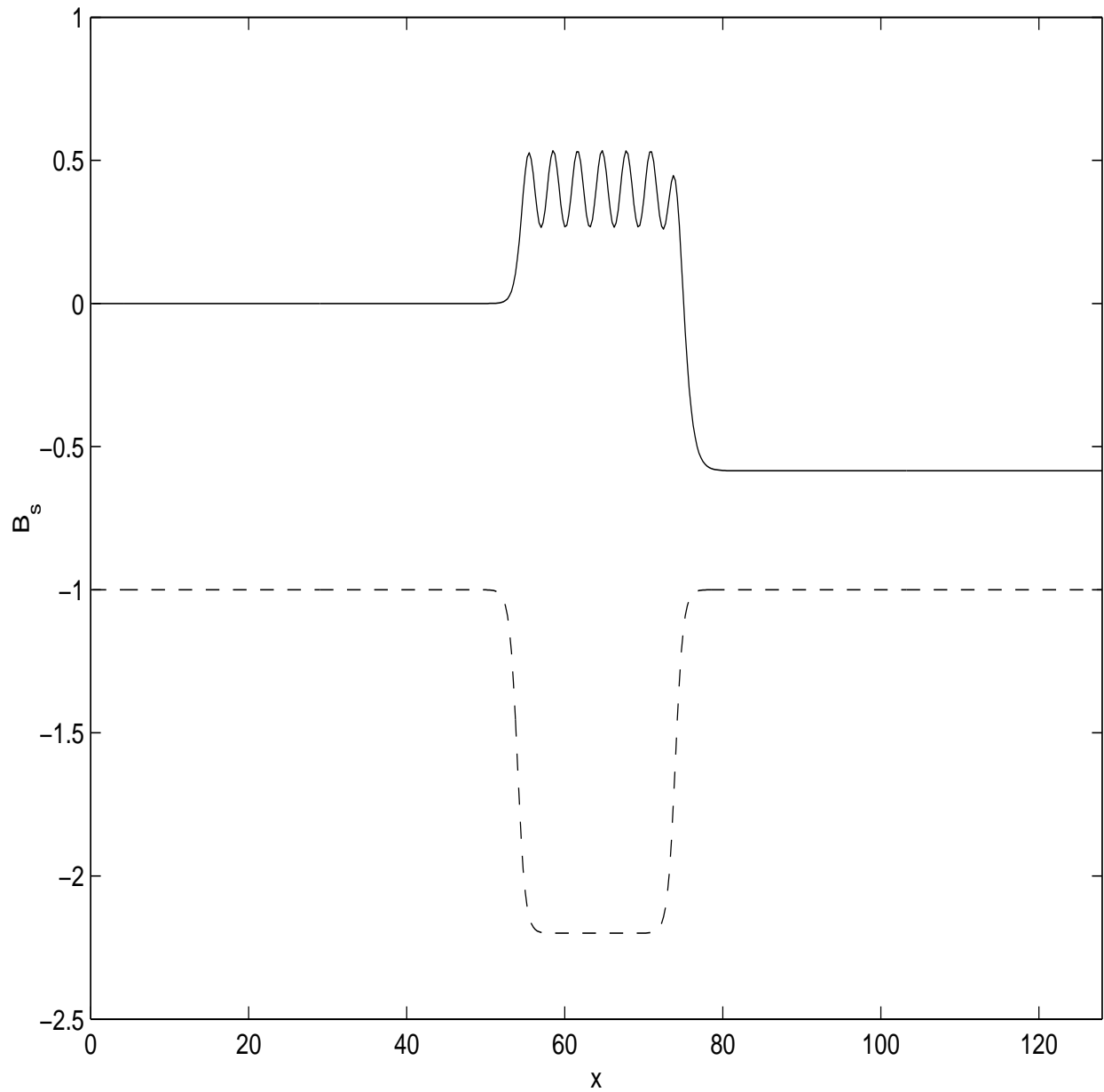


FIG. 1. Numerical solution to (6) (solid line) defined over  $[0, x_u]$  that is centered at  $x_p = x_u/2$  subject to forcing (5) (dash line) where  $L = 20$ ,  $\gamma = 1.2$ ,  $\Delta = 1.753574$  and  $x_u = 128$ . Trapped waves can be seen in the vicinity of the hole.

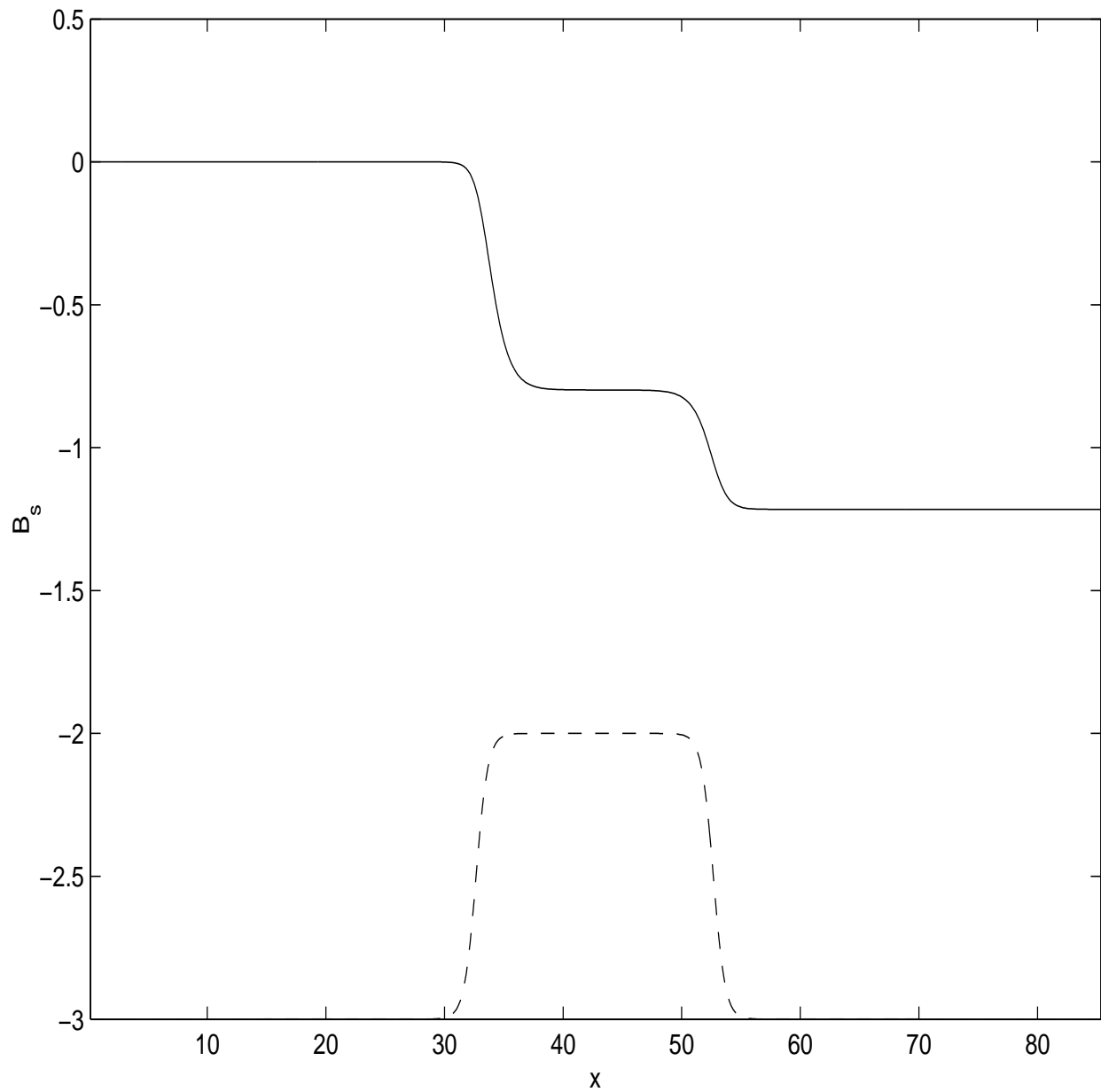


FIG. 2. Numerical solution to (6) (solid line) defined over  $[0, x_u]$  that is centered at  $x_p = x_u/2$  subject to forcing (5) (dash line) where  $L = 20$ ,  $\gamma = -1$ ,  $\Delta = 3.6475$  and  $x_u = 85.33$ .

Steady transcritical flow over a hole

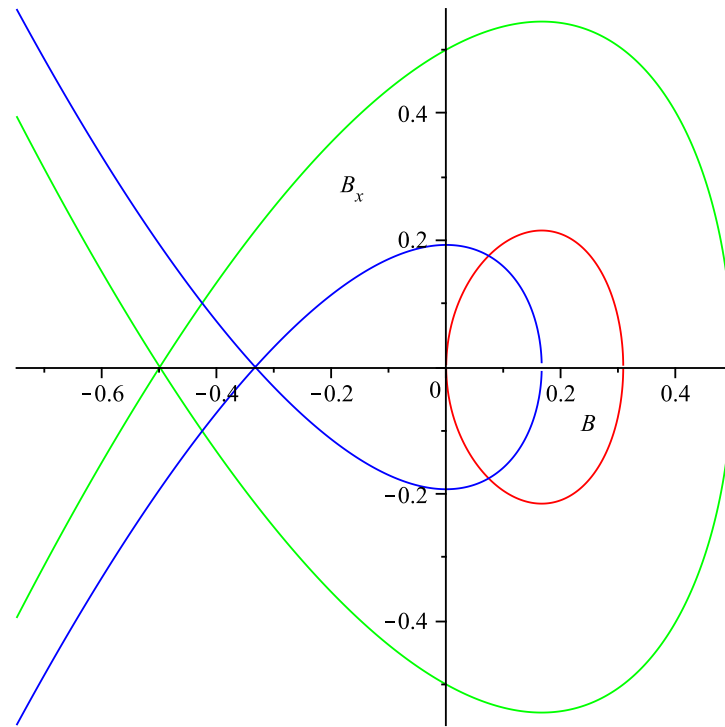


FIG. 3. Phase plane for  $\Delta = 1.0, \gamma = 0.25$ .

## Steady transcritical flow over a hole

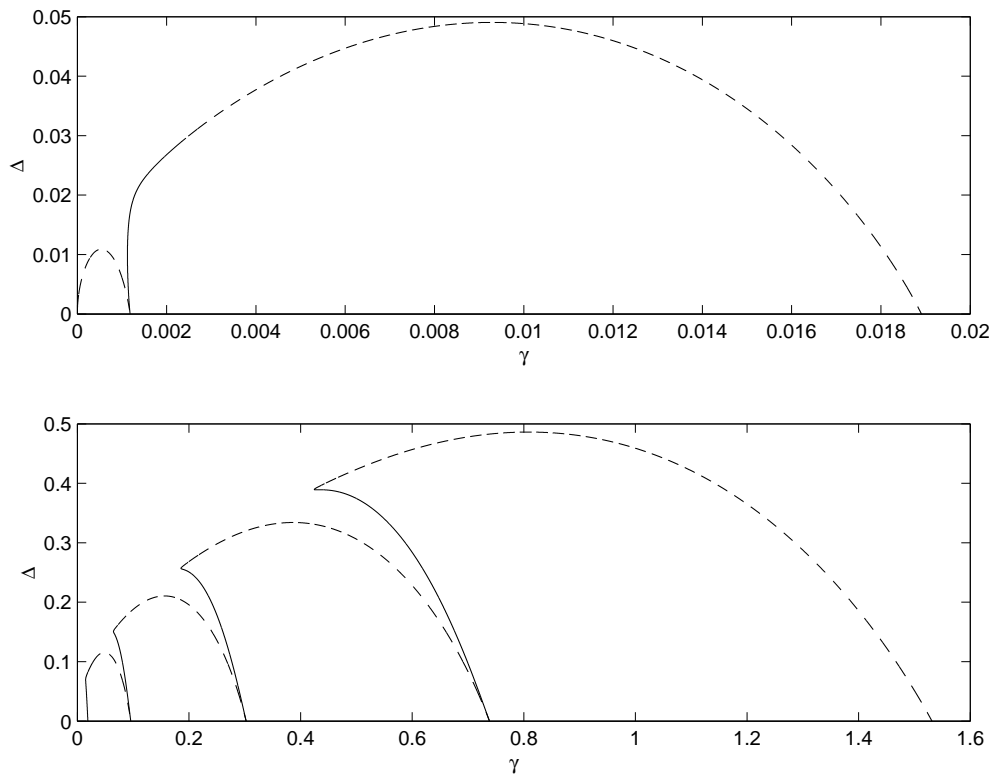


FIG. 4. Parametric map  $\Delta(\gamma)$  given by (22) for the piece-wise constant forcing using  $L = 20$  and  $n = 0, 1, 2, 3, 4, 5$ . Top panel shows the two smallest two loops corresponding to  $n = 0, 1$  whereas the remaining four loops featured in the bottom panel correspond to  $n = 2, 3, 4, 5$ . The second and third loops are connected. The bold and dash lines represent the alternating signs  $\mp$  used in the term  $F(m)$  of (22) respectively.

Steady transcritical flow over a hole

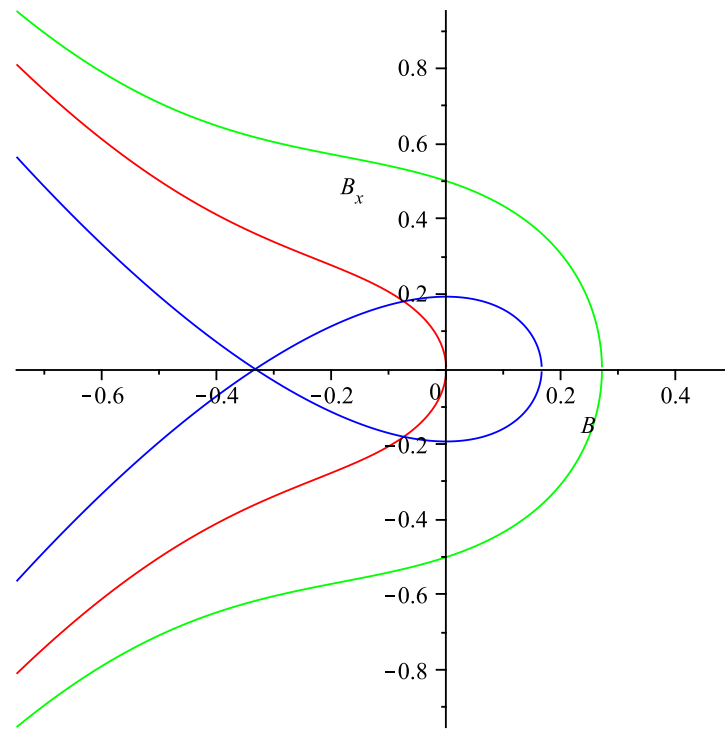


FIG. 5. Phase plane for  $\Delta = 1.0, \gamma = -0.25$ .

## Steady transcritical flow over a hole

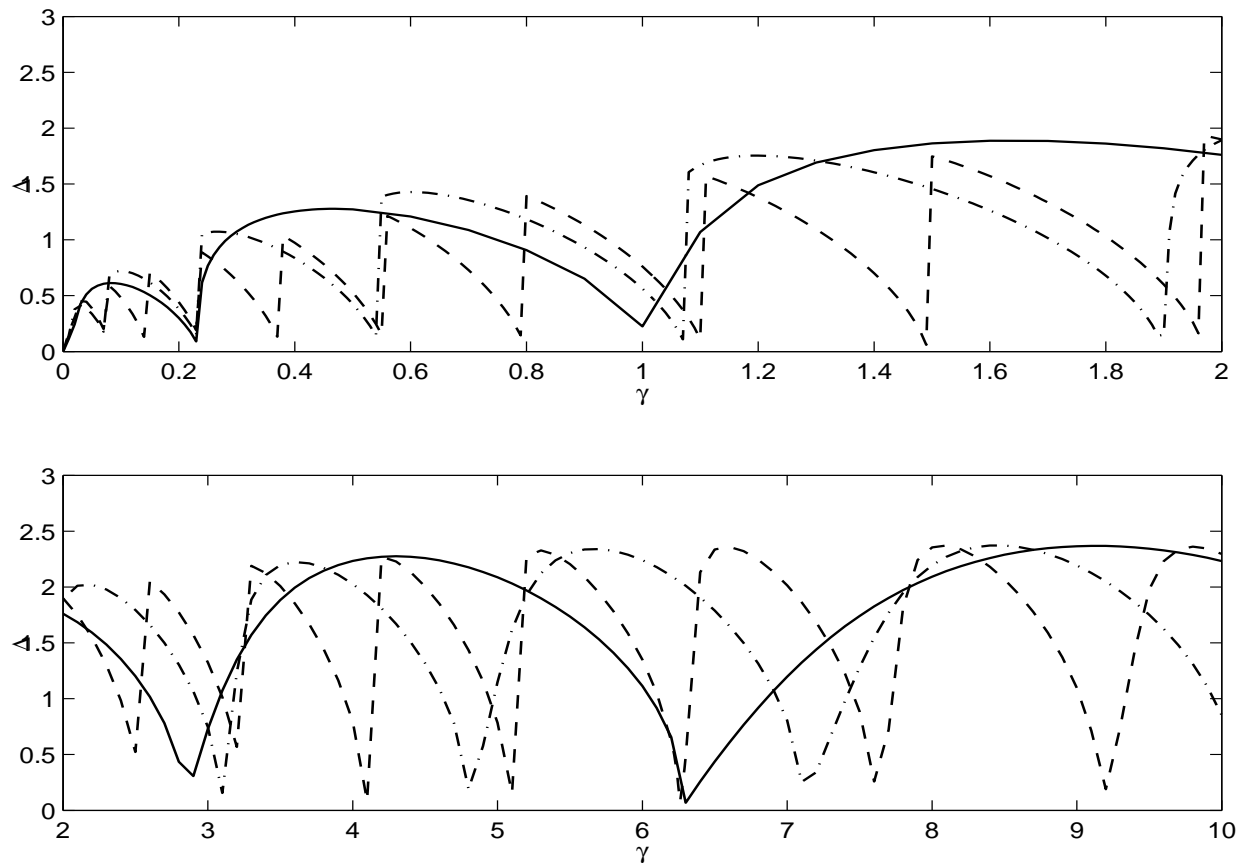


FIG. 6. Parametric Maps of  $\Delta(\gamma)$  leading to steady dispersive hydraulic solutions that solve (6) subject to forcing (5) with  $\Delta x = 1/4$ ,  $\xi = 1$  using  $L = 10$  (bold line),  $L = 20$  (dash-dot) and  $L = 40$  (dash line). Top panel features the two parametric maps for  $0 \leq \gamma \leq 2$  whereas the bottom panel presents the details of the parametric maps for  $2 \leq \gamma \leq 10$ . Upper limit of the parametric map is given by the dashed line in both panels.

## Steady transcritical flow over a hole

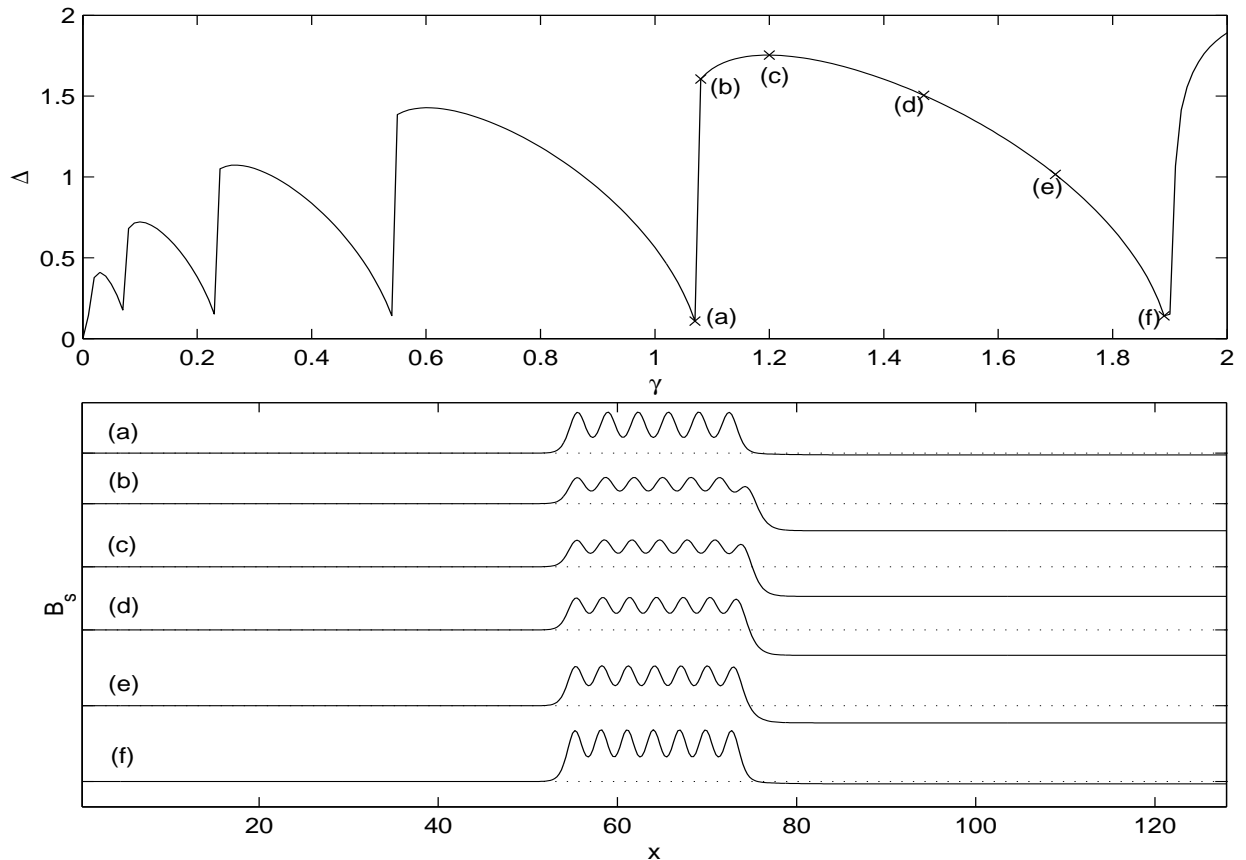


FIG. 7. Top panel: Parametric map of  $\Delta(\gamma)$  leading to steady dispersive hydraulic solutions that solve (6) subject to forcing (5) with  $\Delta x = 1/4$ ,  $\xi = 1$  using  $L = 20$  for  $0 \leq \gamma \leq 2$  along with characteristic points along a single loop at (a)  $\gamma = 1.07$ , (b)  $\gamma = 1.08$ , (c)  $\gamma = 1.20$ , (d)  $\gamma = 1.47$ , (e)  $\gamma = 1.70$  and (f)  $\gamma = 1.89$ . Bottom panel: Plots of numerical solutions to (6) subject to forcing (5) with  $L = 20$  at the characteristic points (a-f) shown in the top panel where the formation of a trapped wave in the vicinity of the hole is shown.

## Steady transcritical flow over a hole

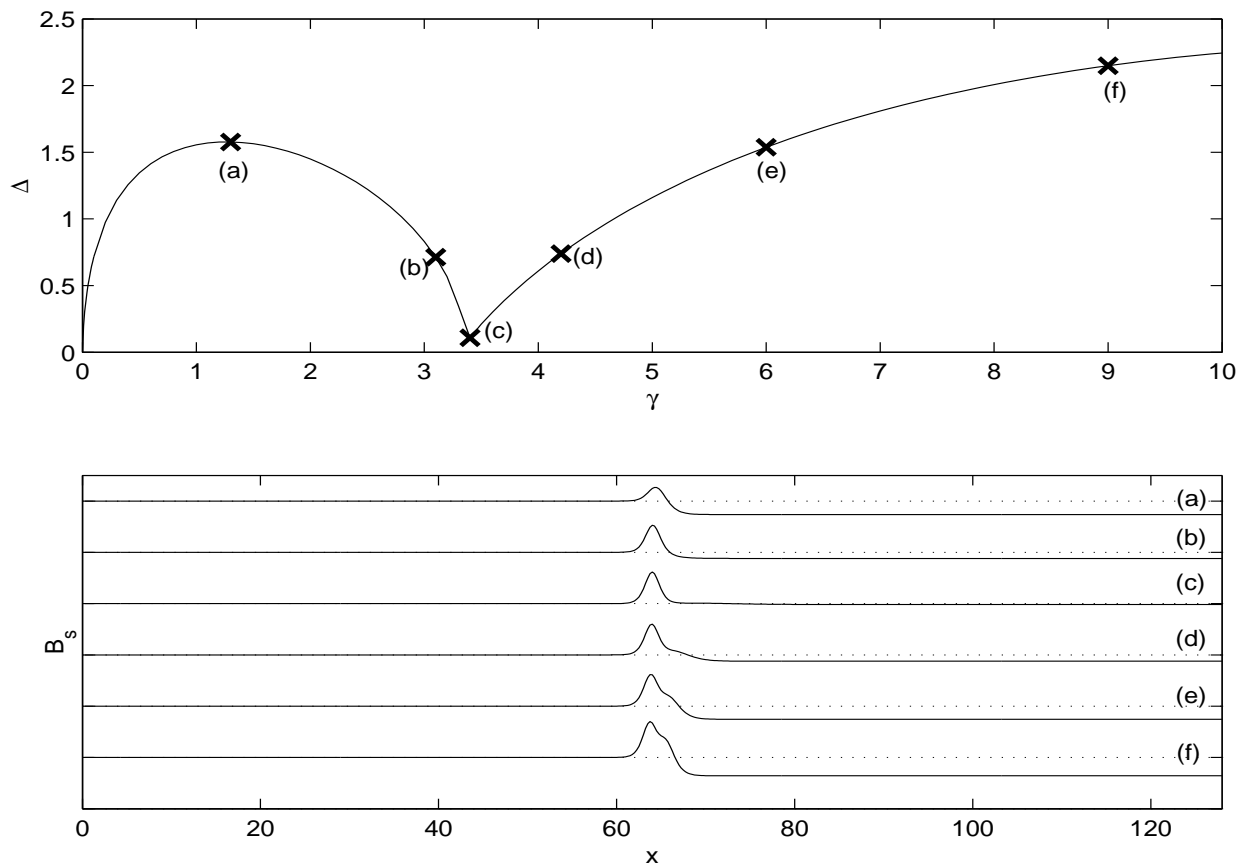


FIG. 8. Top panel: Parametric map of  $\Delta(\gamma)$  leading to steady dispersive hydraulic solutions that solve (6) subject to forcing (5) with  $\Delta x = 1/4$ ,  $\xi = 1$  using  $L = 2$  for  $0 \leq \gamma \leq 10$  along with characteristic points along a single loop at (a)  $\gamma = 1.30$ , (b)  $\gamma = 3.10$ , (c)  $\gamma = 3.40$ , (d)  $\gamma = 4.20$ , (e)  $\gamma = 6$  and (f)  $\gamma = 9$ . Bottom panel: Plots of numerical solutions to (6) subject to forcing (5) with  $L = 2$  at the characteristic points (a-f) shown in the top panel where the widening of the steady hydraulic solution is shown.

# Steady transcritical flow over a hole

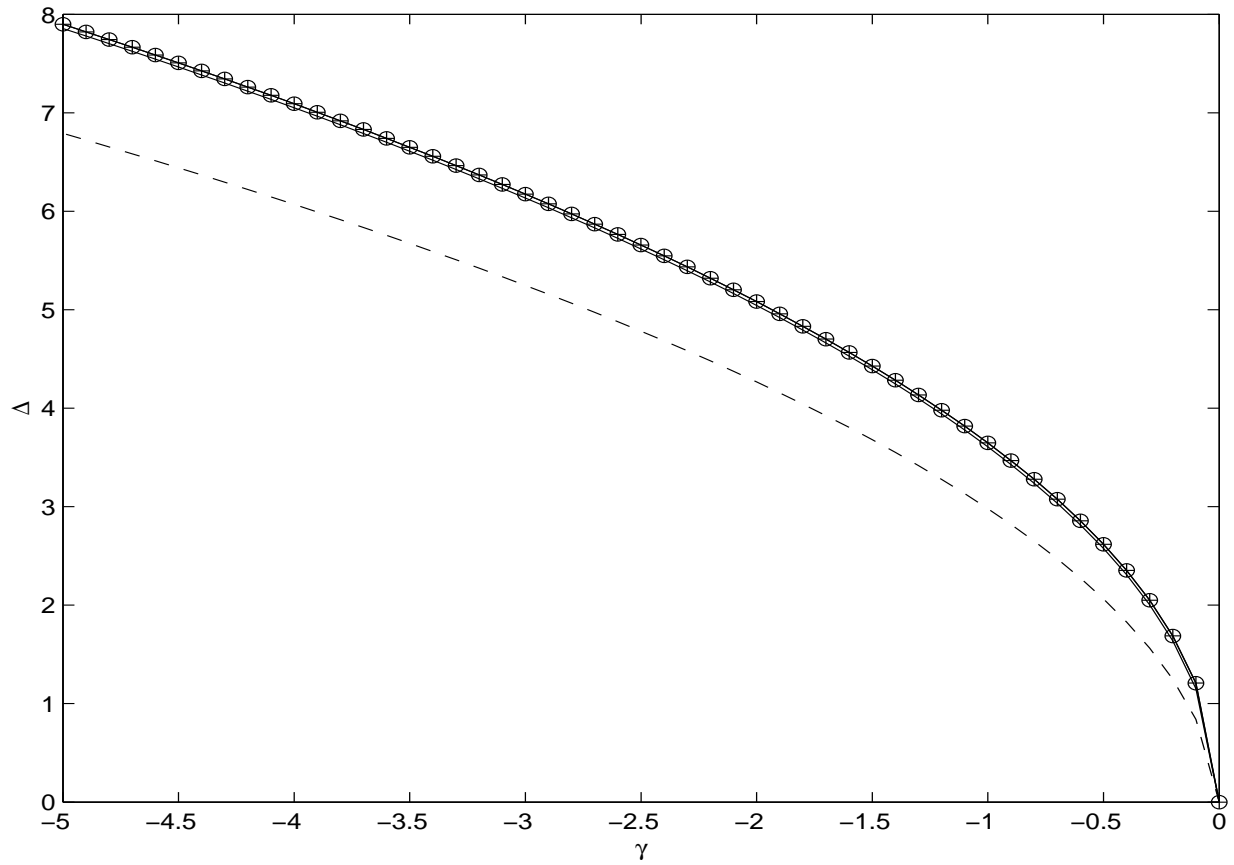


FIG. 9. Parametric Maps of  $\Delta(\gamma)$  leading to steady dispersive hydraulic solutions that solve (6) subject to forcing (5) with  $\Delta x = 1/6$ ,  $\xi = 1$  using  $L = 2$ (dash),  $L = 5$  (bold),  $L = 10$  (bold line with circle) and  $L = 20$  (bold line with cross) for  $-5 \leq \gamma \leq 0$ .

# Steady transcritical flow over a hole

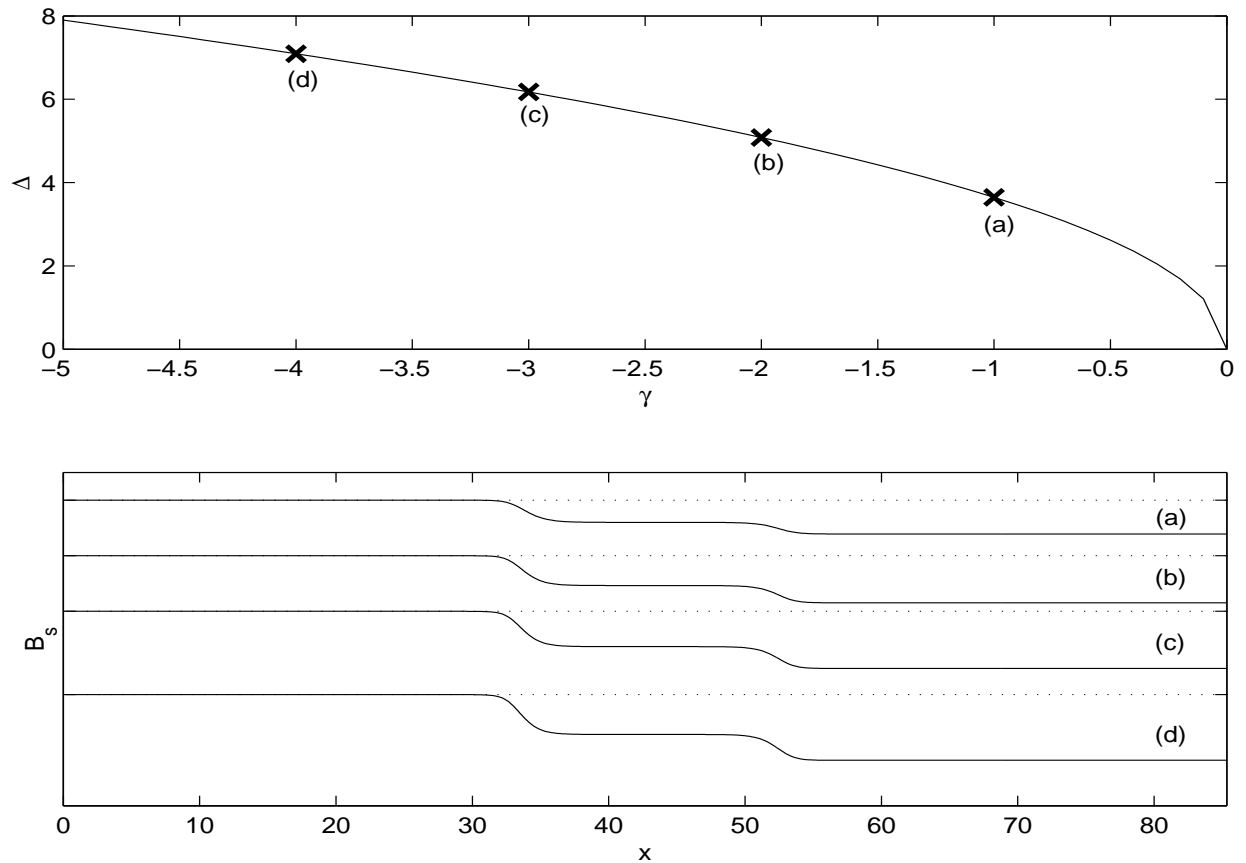


FIG. 10. Top panel: Parametric map of  $\Delta(\gamma)$  leading to steady dispersive hydraulic solutions that solve (6) subject to forcing (5) with  $\Delta x = 1/6$ ,  $\xi = 1$  using  $L = 20$  for  $-5 \leq \gamma \leq 0$  along with characteristic points along a single loop at (a)  $\gamma = -1$ , (b)  $\gamma = -2$ , (c)  $\gamma = -3$  and (d)  $\gamma = -4$ . Bottom panel: Plots of numerical solutions to (6) subject to forcing (5) with  $L = 20$  at the characteristic points (a-d) shown in the top panel.

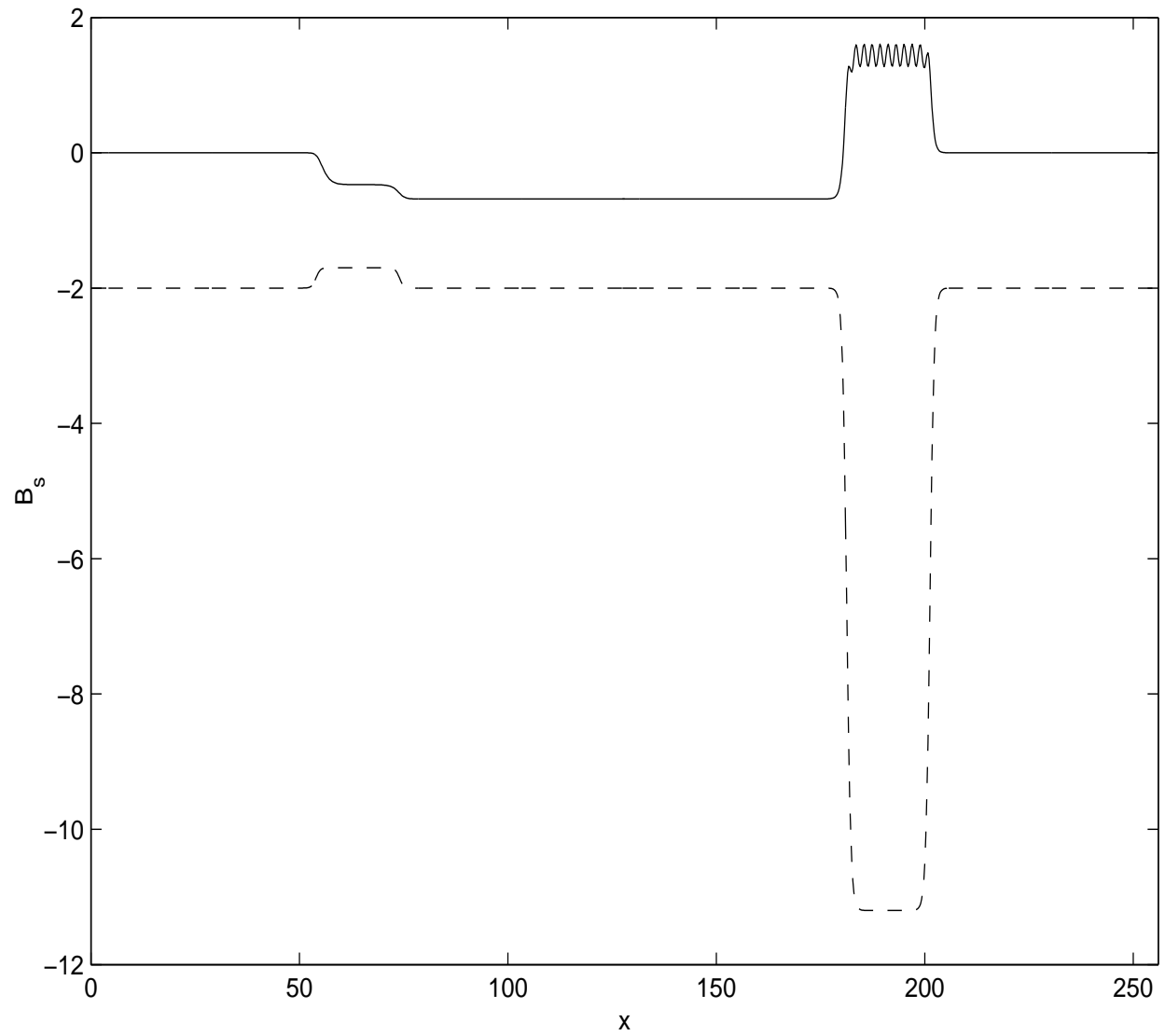


FIG. 11. Numerical solution of the forced KdV equation (6) (solid line) for a plateau located at  $x_p = 64$  and a hole located at  $x_p = 196$ ,  $\Delta = 2.05$  and the respective forcing amplitudes are  $\gamma = -0.3$  and  $\gamma = 9.2$ .